Supplementary Material

4D Printing of Programmable Liquid-Vapor Phase Change Composites for Multi-Responsive Flexible Actuators

Hongru Zheng[a,c,1], Mingquan Fang[b,c,1], Fei Long[c], Huilan Jing[b,c], Bing Wang[b,c], Xunye Fan[c], Jianjun Guo[c], Yuchuan Cheng[b,c*], Aihua Sun[c*]

a. School of Materials Science and Chemical Engineering, Ningbo University, Ningbo 315211, P. R. China

b. Center of Materials Science and Optoelectronics Engineering, University of Chinese Academy of Sciences, Beijing 100049, P. R. China

c. Laboratory of Atomic-scale and Micro & Nano Manufacturing, Ningbo Institute of Materials Technology & Engineering, Chinese Academy of Sciences, Ningbo 315201, P. R. China

* Corresponding authors.
E-mail addresses: yccheng@nimte.ac.cn

[1]These authors contributed equally to this work.

List of Contents

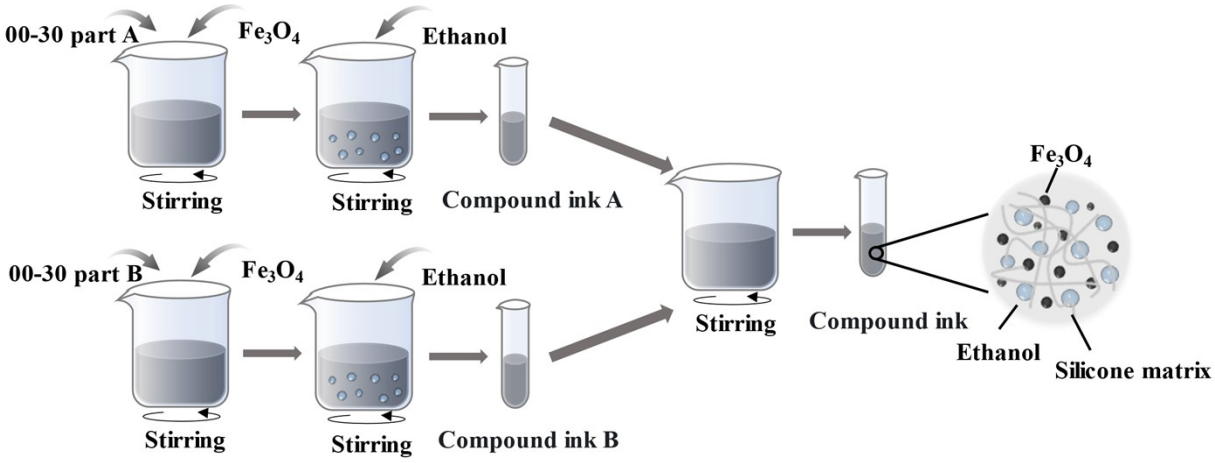

Figure S1. Fabrication process of the of magnetocaloric responsive liquid-vapor phase transition elastomers inks.

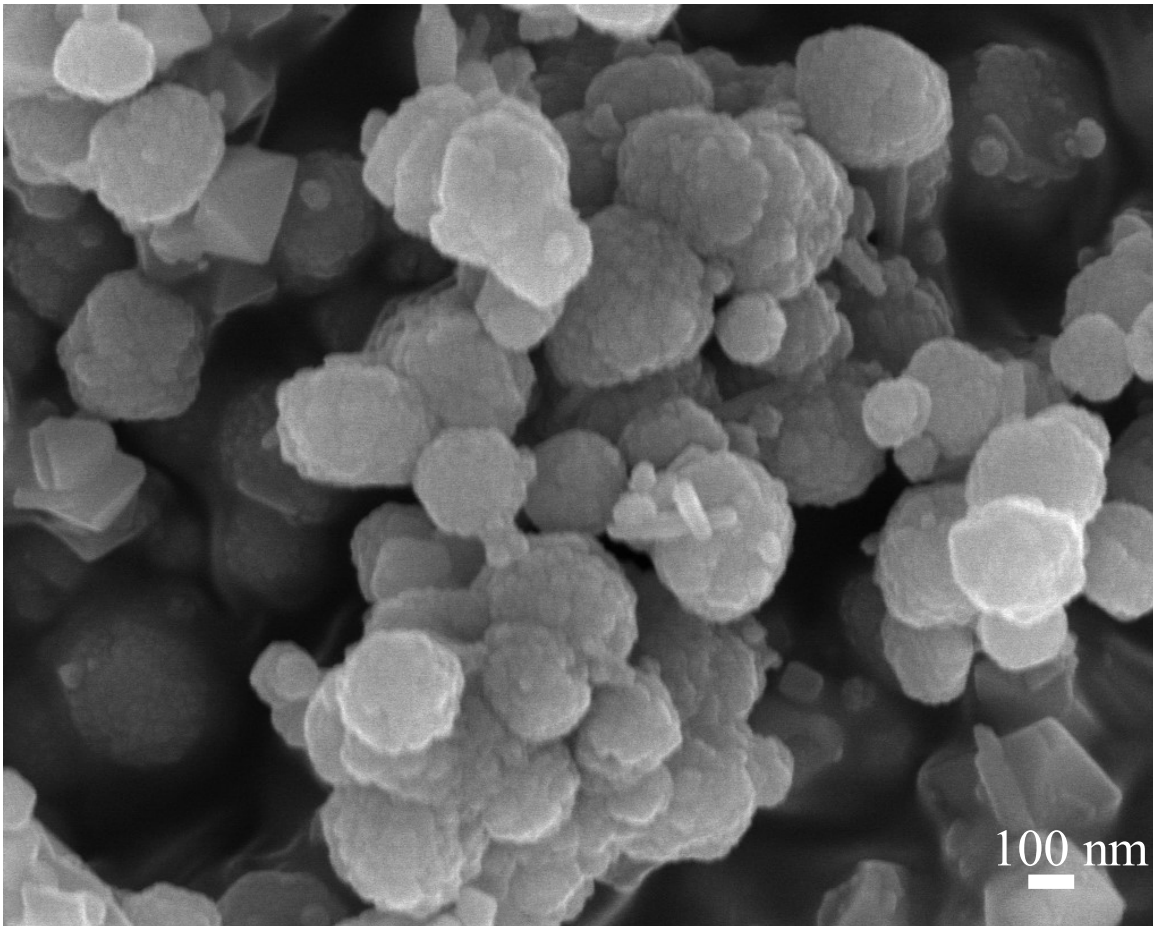

Figure S2. TEM image of Fe_3O_4 nanoparticles

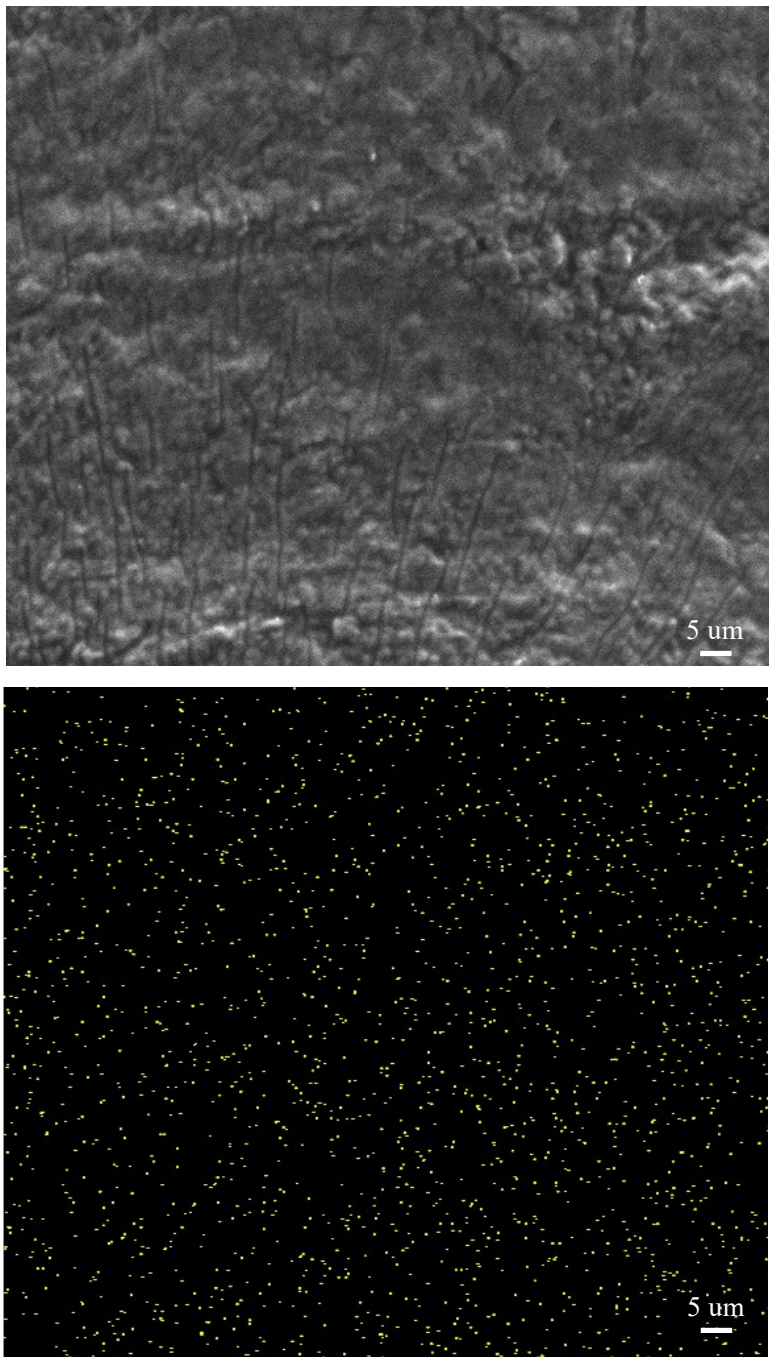

Figure S3. Elemental analysis of Fe_3O_4 dispersed in silicone rubber.

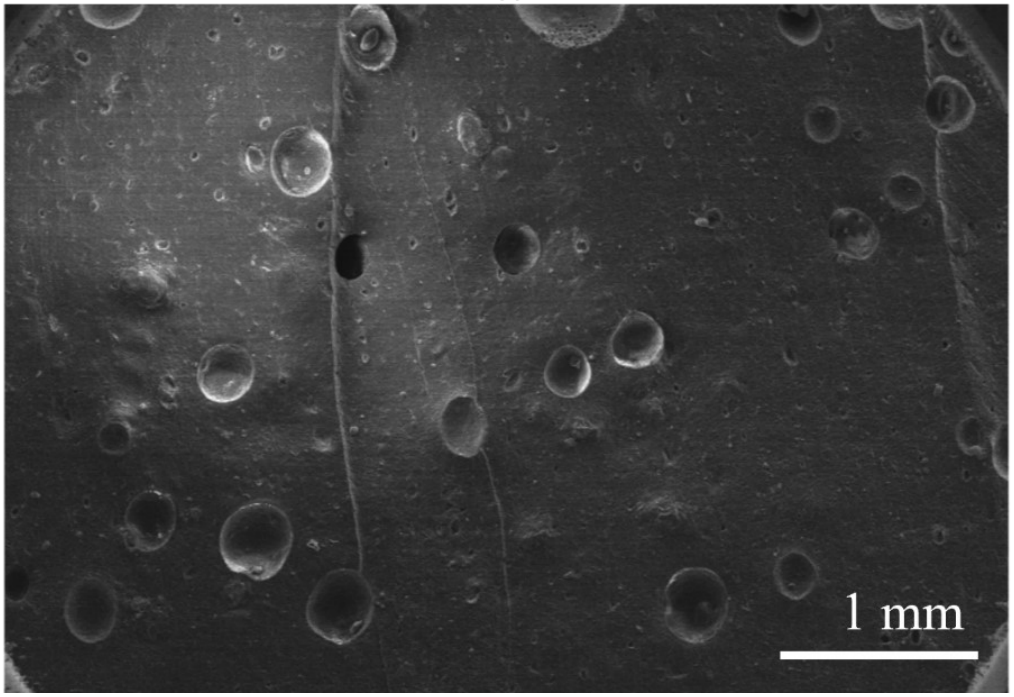

Figure S4 Ethanol micro-cavities inside elastomers

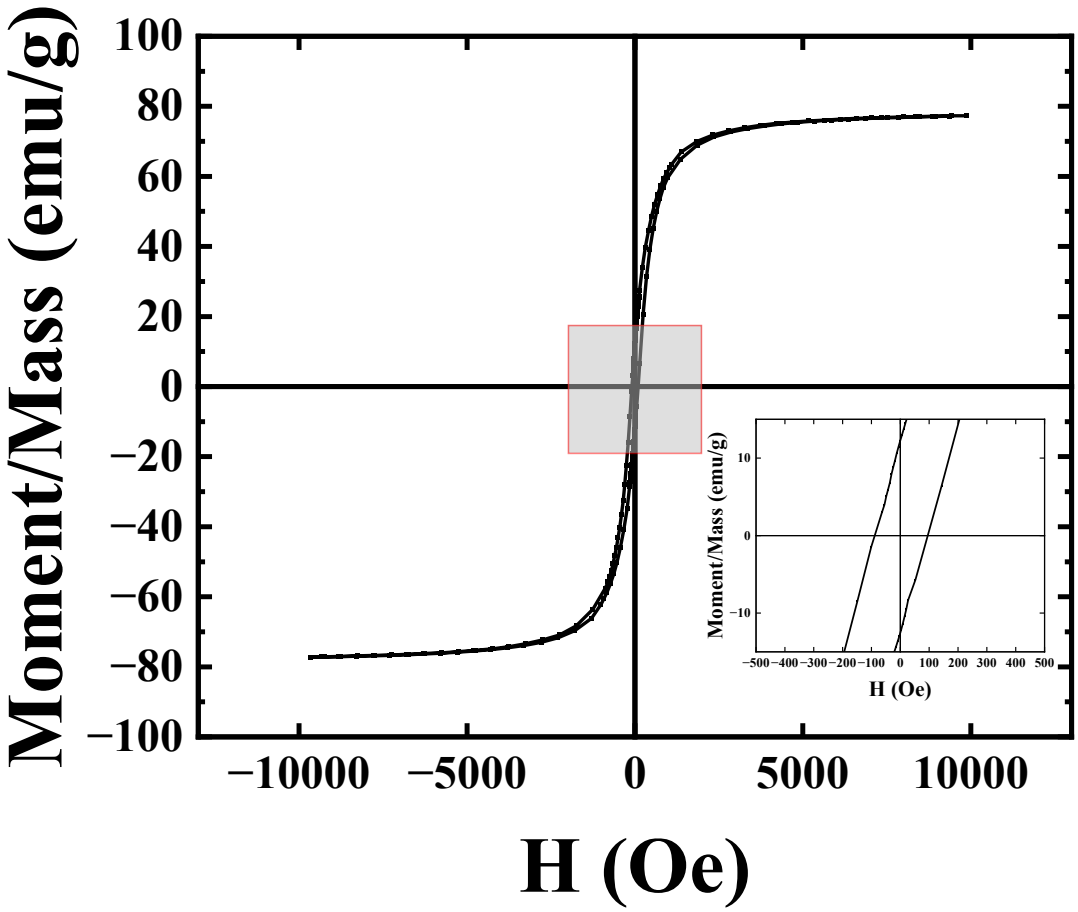

Figure S5. Magnetic hysteresis loop diagrams of Fe_3O_4.

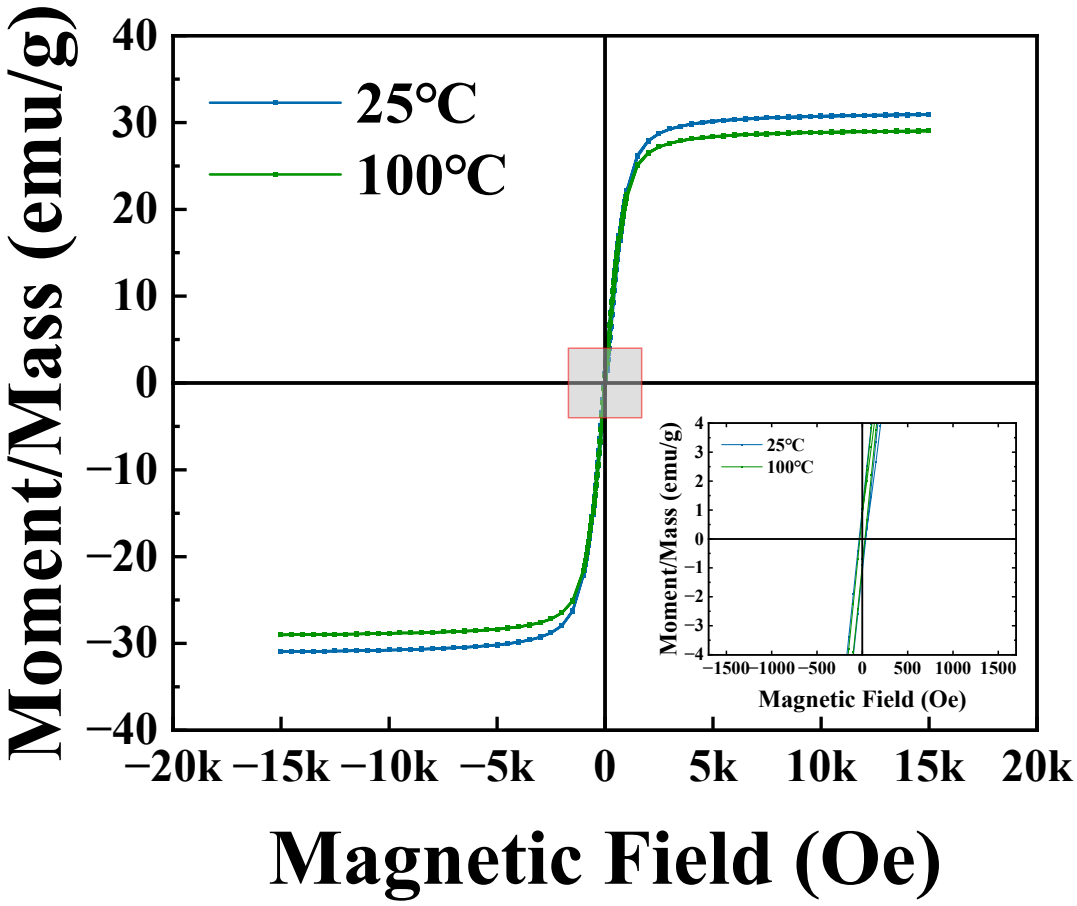

Figure S6. Magnetic hysteresis loop diagrams of composite materials at 25 °C and 100 °C.

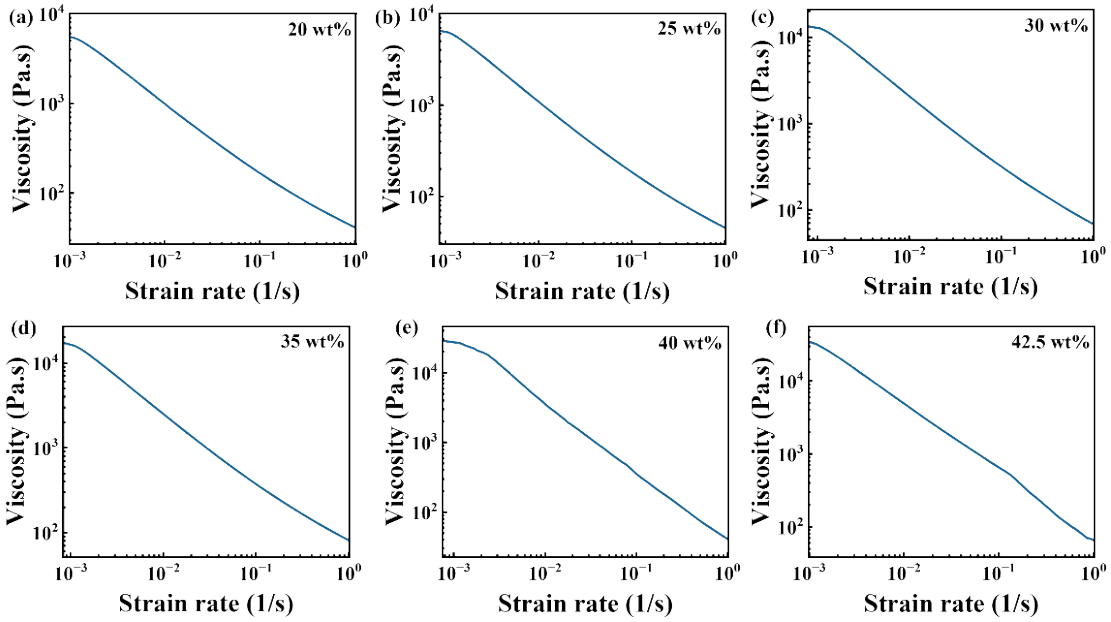

Figure S7. Viscosity with Fe_3O_4 content ranging from 20 % to 42.5 %.

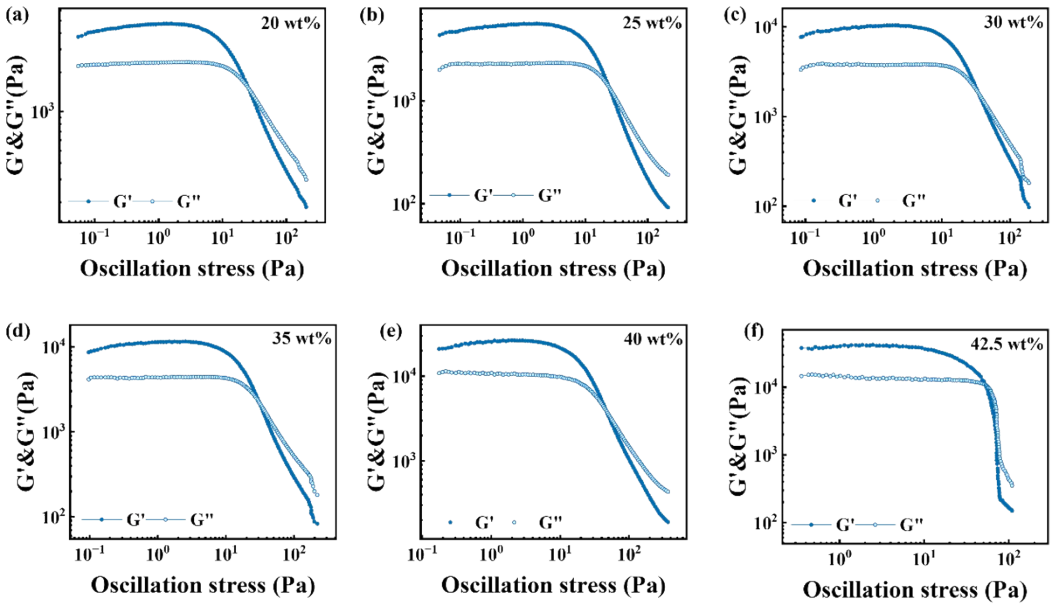

Figure S8. Modulus with Fe_3O_4 content ranging from 20 % to 42.5 %.

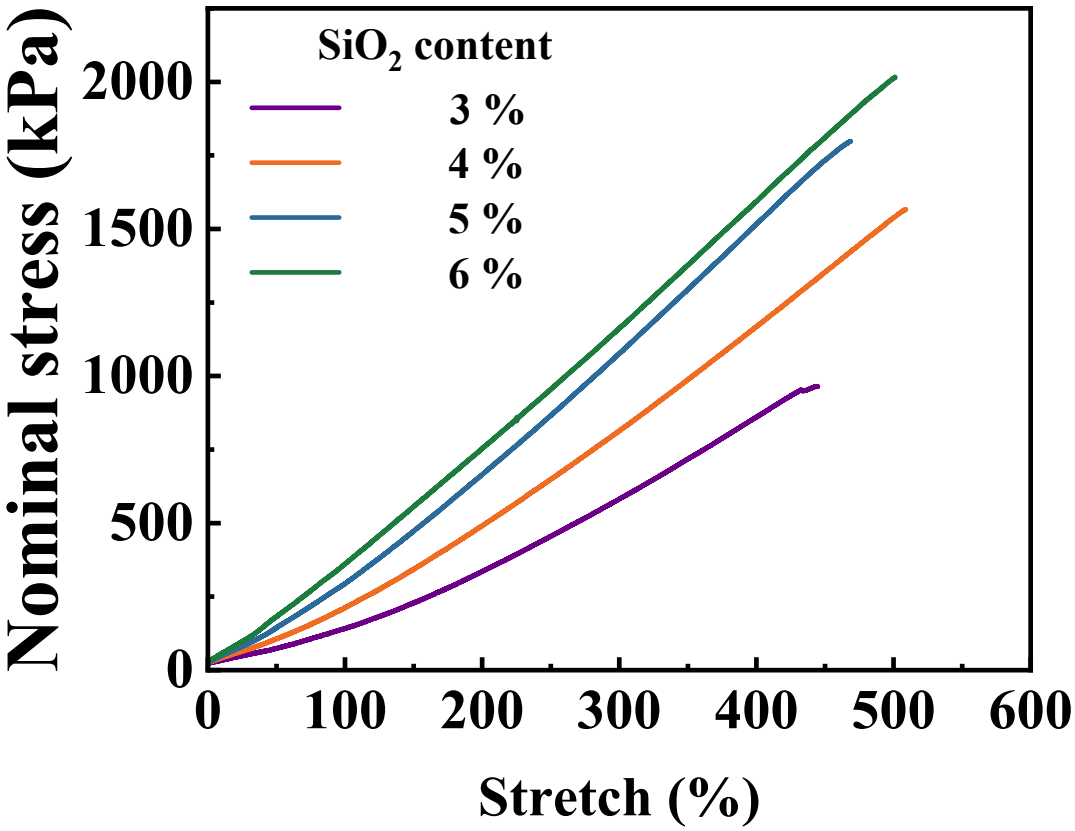

Figure S9. Mechanical properties of I-shaped specimens with different SiO_2 contents. When the SiO_2 content exceeds 6 wt%, the SiO_2 powder cannot fully blend with the 00-50.

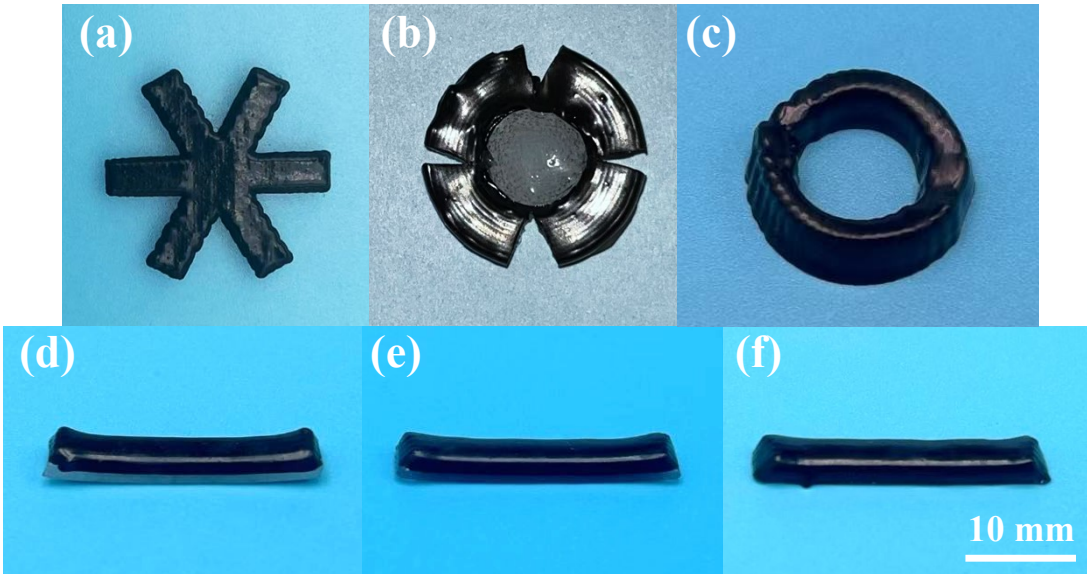

Figure S10. Photographs of liquid-gas phase transition actuators.

The ratio of the active layer to the passive layer in figure (d), (e), (f) are 1:1, 2:1 and 5:1 respectively.